C. R. Chimie xxx (2013) xxx–xxx

Contents lists available at SciVerse ScienceDirect

Comptes Rendus Chimie

www.sciencedirect.com

Full paper/Mémoire

Synthesis of bis *N*-heterocyclic carbenes, derivatives and metal complexes

Arlanda Huffer, Ben Jeffery, Benjamin J. Waller, Andreas A. Danopoulos *

Laboratoire de chimie de coordination, Institut de chimie (UMR 7177 CNRS), université de Strasbourg, 4, rue Blaise-Pascal, 67081 Strasbourg, France

ARTICLE INFO

Article history:
Received 19 October 2012
Accepted after revision 24 January 2013
Available online xxx

Keywords:
N-heterocyclic carbenes
Tellurium
Palladium
Platinum
Nickel
Iridium
Crystal structures

ABSTRACT

A method for the synthesis and isolation of 1,1′-methylene-bis-(3-aryl-imidazol-2-ylidene) ligands, aryl = 2,6-di*iso*propyl-phenyl (DiPP), $\mathbf{L^{DiPP}}$, mesityl (mes), $\mathbf{L^{mes}}$, is reported, which provides synthetically useful quantities of high purity. Derivatisation of $\mathbf{L^{DiPP}}$ with chalcogenides gave the adducts $\mathbf{L^{DiPP}E_2}$, E = S, Se, Te. Reaction of $\mathbf{L^{DiPP}}$ with $[Pd(tmeda)Me_2]$, $[Pt(\mu\text{-}SMe_2)Me_2]_2$, $[Ir(1,5\text{-}COD)(\mu\text{-}Cl)]_2/KPF_6$ and $[NiBr_2(dme)]$ gave $[Pd(L^{DiPP})Me_2]$ (**1**), $[Pt(L^{DiPP})Me_2]$ (**2**), $[Ir(L^{DiPP})(1,5\text{-}COD)](PF_6)$ (**3**) and $[Ni(L^{DiPP})Br_2]$ (**4**), respectively. The latter was reduced in the presence of CO to $[Ni(L^{DiPP})(CO)_2]$ (**5**). The structures of $\mathbf{L^{mes}}$, $\mathbf{L^{DiPP}Te_2}$, and **1**–**5** are also reported.

© 2013 Published by Elsevier Masson SAS on behalf of Académie des sciences.

RÉSUMÉ

Nous décrivons une méthode de synthèse des ligands bis-carbènes 1,1′-méthylène-bis-(3-aryl-imidazol-2-ylidène) (aryl = 2,6-di*iso*propyl-phényl (DiPP), $\mathbf{L^{DiPP}}$; mésityl (mes), $\mathbf{L^{mes}}$) qui permet de les isoler en grandes quantités et haute purité. La réaction de $\mathbf{L^{DiPP}}$ avec les chalcogénures a conduit aux dérivés $\mathbf{L^{DiPP}E_2}$, E = S, Se, Te. Les réactions de $\mathbf{L^{DiPP}}$ avec $[Pd(tmeda)Me_2]$, $[Pt(\mu\text{-}SMe_2)Me_2]_2$, $[Ir(1,5\text{-}COD)(\mu\text{-}Cl)]_2/KPF_6$ et $[NiBr_2(dme)]$ ont donné respectivement $[Pd(L^{DiPP})Me_2]$ (**1**), $[Pt(L^{DiPP})Me_2]$ (**2**), $[Ir(L^{DiPP})(1,5\text{-}COD)](PF_6)$ (**3**) et $[Ni(L^{DiPP})Br_2]$ (**4**). Ce dernier fut réduit en présence de CO en $[Ni(L^{DiPP})(CO)_2]$ (**5**). Les structures de $\mathbf{L^{mes}}$, $\mathbf{L^{DiPP}Te_2}$, and **1**-**5** sont également décrites.

© 2013 Publié par Elsevier Masson SAS pour l'Académie des sciences.

1. Introduction

Chelating bis-*N*-heterocyclic carbene (NHC) complexes followed as early developments after the introduction of the NHC functionality in the coordination chemistry, which gained momentum with the isolation of 'bottleable' NHCs by Arduengo [1]. Bis-imidazolium salts linked by alkylene spacers served as precursors to the corresponding NHCs and proved the reagents of choice as in situ sources of the NHC ligands leading to the synthesis of Pd complexes [2].

Since then, chelating dicarbene ligands (Scheme 1) have been studied mainly on Pd and Pt centres due to the emerging potential of the corresponding complexes in homogeneous catalysis (cross coupling, copolymerisation, carbonylation, C–H activation, CO_2 activation), [3] stabilisation of high oxidation states [4] and, more recently, photophysical applications [5]. Other metals have not been studied as extensively. Early work on Ni demonstrated the potential of Ni-NHC complexes in catalysis [6], and on Cr the stabilisation of organometallics of relevance to alkene polymerisation and oligomerisation [7]. In most cases, the commonly used ligand with a methylene spacer between the heterocyclic donors (Scheme 1 **A**–**C**) is not being isolated, but introduced to the metal centre by the reaction with metal precursors coordinated to an internal base

* Corresponding author.
E-mail address: danopoulos@unistra.fr (A.A. Danopoulos).

1631-0748/$ – see front matter © 2013 Published by Elsevier Masson SAS on behalf of Académie des sciences.
http://dx.doi.org/10.1016/j.crci.2013.01.016

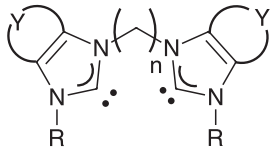

R = alkyl, n = 1, Y = $(H)_2$ (**A**) or $(CH)_4$ (**B**)
R = mes, DiPP, n = 1, Y = $(H)_2$ (**C**): This work

Scheme 1.

(e.g. acetate, acac, etc.), or by deprotonating the di-imidazolium precursors in situ with an external base (NaOAc, Et_3N) in the presence of a suitable metal precursor.

Attempts to isolate the free di-NHC ligand have been reported for type **A** ligands (R = Bu,^{t} [6a] benzyl [6b]). In addition, the ligand of type **C** (R = DiPP) has been prepared by deprotonation of the corresponding imidazolium salt with $KN(SiMe_3)_2$ in THF at room temperature [7]. This method, albeit attractive, proved in our hands problematic leading to intensely colored and spectroscopically impure materials, which we were unable to purify by common methods. On the other hand, the advantage of the product stoichiometry control provided by the bulky ligands of type **C** (i.e. formation of complexes with ligand-to-metal stoichiometry 1:1 rather 2:1, the latter being common with NHC ligands of type **A**), prompted us to reinvestigate and expand the synthetic methodology to access the aforementioned ligands of type **C**. In this paper we describe an improved synthesis of ligands $\mathbf{L^{mes}}$ and $\mathbf{L^{DiPP}}$ in synthetically useful quantities and high purity. We also provide some examples of novel transition metal organometalllics that demonstrate some advantages of using the free ligands in synthesis by simple substitution reactions. A summary of the chemical transformations is given in Scheme 2.

2. Results and discussion

2.1. Synthesis of ligands and derivatives

The bis-imidazolium salts $\mathbf{(L^{mes}H_2)Br_2}$ and $\mathbf{(L^{DiPP}H_2)Br_2}$ were prepared by adaptation of established literature procedures [3d,7,8]. Analytically pure, colourless solids were obtained after washing the precipitated products that were formed by the quaternisation of the imidazoles with CH_2Br_2 in xylenes, with small amounts of acetone. For structural characterisation of the $(L^{DiPP}H_2)^{2+}$, $\mathbf{(L^{DiPP}H_2)Br_2}$ was converted to the triflate salt and crystallised from CH_2Cl_2/petrol. The structure of the dication in $\mathbf{(L^{DiPP}H_2)(OTf)_2}$ determined crystallographically is depicted in Fig. 1. It is worth commenting on some differences observed in the structure of the $\mathbf{(L^{DiPP}H_2)(OTf)_2}$ and the known $\mathbf{(L^{DiPP}H_2)Br_2 \cdot H_2O}$ [7]. The vectors of the two C–H imidazolium bonds in the former are pointing to the same direction; this is certainly due to the formation of H-bonding between these C–*H* hydrogen atoms with one oxygen atom of the triflate anion. The interaction may also influence the angle between the two heterocycles

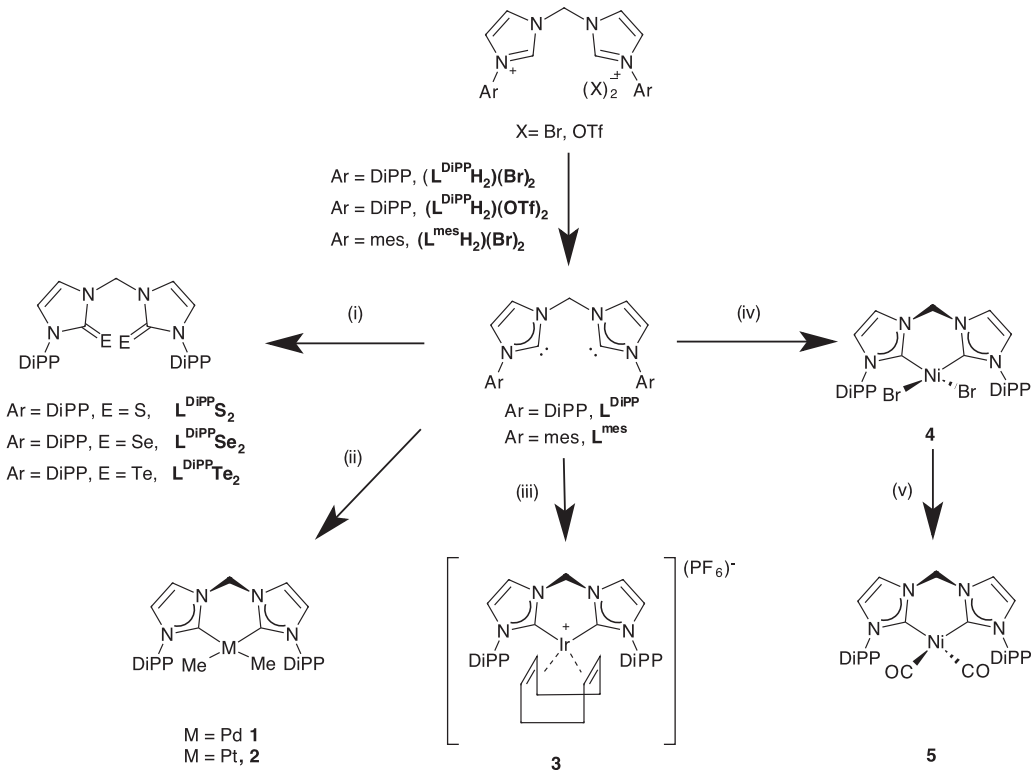

Scheme 2. Synthetic transformations leading to the ligands, derivatives and complexes described in this paper. Reagents: (i) S_8, Se or Te; (ii) $[Pd(tmeda)Me_2]$ (M = Pd); $[Pt(\mu\text{-}SMe_2)Me_2]_2$ (M = Pt); (iii) $[Ir(1,5\text{-}COD)(\mu\text{-}Cl)]_2/KPF_6$; (iv) $[NiBr_2(dme)]$; (v) Na(Hg)/CO.

Please cite this article in press as: Huffer A, et al. Synthesis of bis *N*-heterocyclic carbenes, derivatives and metal complexes. C. R. Chimie (2013), http://dx.doi.org/10.1016/j.crci.2013.01.016

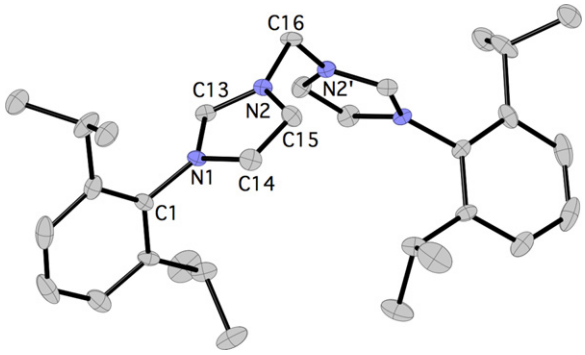

Fig. 1. Representation of the dication in the structure of $(\mathbf{L^{DiPP}H_2})(\mathbf{OTf})_2$; ellipsoids are at 30% probability level. Only one disordered position of one Pr^i groups of one DiPP ring is shown for clarity. Selected bond lengths (Å) and angles (deg): C13–N1 1.332(6), C13–N2 1.329(7), N2–C13–N1 108.4(4), N2–C16–N2′ 110.1(6), N2–C13–N1 108.4(4).

(75.20°) and the N2-C16-N2′ angles. The vectors of the two C–H imidazolium bonds in the $(\mathbf{L^{DiPP}H_2})\mathbf{Br_2}\cdot\mathbf{H_2O}$ are pointing to opposite directions, being involved in H-bonding with different Br^- in the lattice. Lastly, the situation in $(\mathbf{L^{mes}H_2})\mathbf{Br_2}$ [9] is analogous with that in the triflate salt mentioned above (i.e. imidazolium C–H vectors are pointing to the same direction and H-bonding with the same Br^-) even though the N-C-N angle at the bridging C atom is *ca.* 112° (*cf. ca.* 110° in $(\mathbf{L^{DiPP}H_2})(\mathbf{OTf})_2$). Therefore, it appears that the relative orientations of the C–H bonds, the interplanar angle between the imidazole heterocycles and the angle at the bridging C atom are dependent on crystal packing and H-bonding interactions between the imidazolium hydrogens and the anion(s).

Prior to the deprotonation reactions described below, the imidazolium salts were dried azeotropically with toluene.

In order to access the free $\mathbf{L^{mes}}$ and $\mathbf{L^{DiPP}}$, the conditions of deprotonation described previously [7] have been modified to suppress product decomposition which is noticeable above −20 °C by the intense brown coloration of the reaction mixture. The decomposition slowed down if the deprotonation was carried out in diethyl ether and the product when dissolved or suspended was maintained below −20 °C. However, after isolation of the product as a solid, it was stable for longer periods (at least 0.5 h) at room temperature under inert atmosphere without appreciable visual or spectroscopic (^{1}H-NMR) change. We were unable to establish the nature of the colored decomposition product. The off-white to yellow $\mathbf{L^{DiPP}}$ and $\mathbf{L^{mes}}$ were characterised by NMR spectroscopic methods (^{1}H and ^{13}C{^{1}H}). The spectra support a symmetrical structure in solution, while the C_{NHC} in the ^{13}C{^{1}H} spectrum for both ligands appear at *ca.* δ 218. Interestingly, X-ray quality crystals of $\mathbf{L^{mes}}$ were obtained and used for structural determination by crystallography. Due to the poor crystal quality as evidenced from the observation of low diffraction angles, the data set was finally collected at the Daresbury synchrotron facility, and was suitable to establish the unit cell contents and atom connectivity and extract metrical data with reasonable accuracy. A diagram of the molecule is shown in Fig. 2.

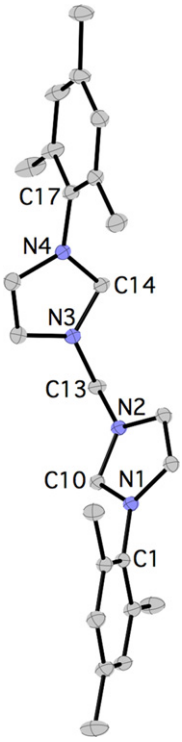

Fig. 2. Representation of the structure of $\mathbf{L^{mes}}$; ellipsoids are at 30% probability level. Selected bond lengths (Å) and angles (deg): N1–C10 1.3702(12), N2–C10 1.3617(12), N3–C14 1.3674(12), N4–C14 1.3646(13), N2–C10–N1 101.56(8), N3–C13–N2 112.02(8), N4–C14–N3 101.50(8).

The molecule adopts a conformation where the lone pairs at C_{NHC} are pointing towards opposite directions, with an interplanar angle between the heterocycles of 77.85°. In addition, there is a reduction of the size of the angles at the C_{NHC} compared to the corresponding angles in the imidazolium salts.

Derivatisation of the NHCs by the reaction with chalcogens has been used as a chemical diagnostic method for their transient presence and characterisation of free NHCs and their indirect structural identification. The most commonly employed chalcogen for this purpose is S_8 leading to air stable thioureas. Less stable selenoureas and telluroureas are expected from the reaction with Se and Te, respectively. Taking advantage of this methodology in order to confirm the successful preparation of the free NHC ligands as detailed above, we reacted the isolated $\mathbf{L^{DiPP}}$ with S_8, Se and Te and obtained the corresponding ureas that were characterised spectroscopically and analytically. In addition, the structure of the telluro-urea $\mathbf{L^{DiPP}Te_2}$ was determined crystallographically and is shown in Fig. 3. It constitutes a rare example of structurally characterised compound of this type [10].

The heterocyclic rings arrange at a dihedral angle of 45.12°, while the C=Te vectors have an *anti*orientation. The C_{Te}–N bond lengths are virtually identical with the corresponding C_{NHC}–N in the free NHC, however the values of the endocyclic angle at the C_{Te} are significantly larger than the corresponding at the C_{NHC}, which may

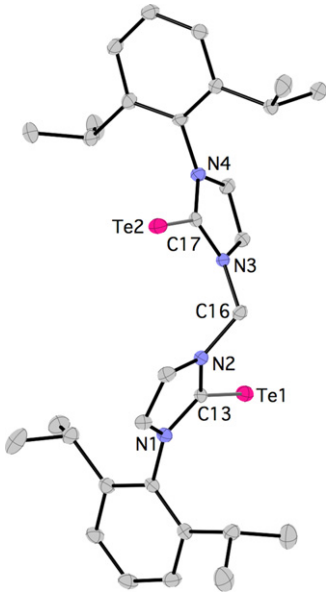

Fig. 3. Representation of the structure of $\mathbf{L^{DiPP}Te_2}$; ellipsoids are at 30% probability level. One molecule of crystallisation solvent C_6D_6 in the asymmetric unit is omitted for clarity. Selected bond lengths (Å) and angles (deg): C13–N1 1.370(6), C13–N2 1.371(6), C13–Te1 2.065(5), C17–N4 1.353(6), C17–N3 1.373(6), C17–Te2 2.073(5), N2–C13–N1 108.4(4), N2–C16–N3 116.4(3), N4–C17–N3 105.3(4).

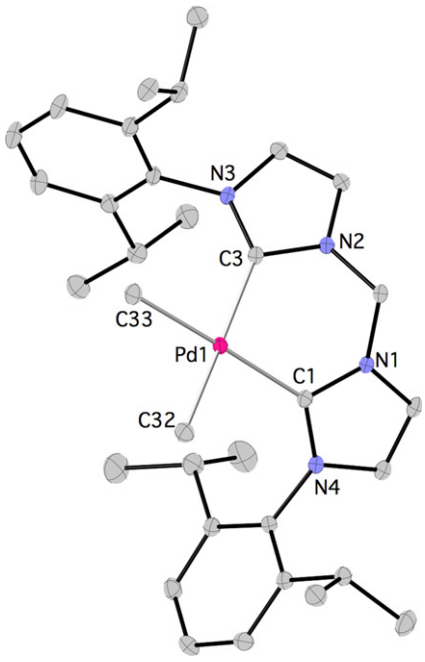

Fig. 4. Representation of the structure of **1**; ellipsoids are at 30% probability level. One disordered THF molecule in the asymmetric unit is omitted for clarity. Selected bond lengths (Å) and angles (deg): C1–N1 1.361(3), C1–N4 1.361(3), C1–Pd1 2.071(2), C3–Pd1 2.065(2), C3–N3 1.375(3), C3–N2 1.372(3), C32–Pd1 2.069(2), C33–Pd1 2.074(2), C3–Pd1–C1 87.95(8), C32–Pd1–C1 94.04(9), C32–Pd1–C33 85.33(9), C3–Pd1–C33 92.75(9).

indicate a varying degree of π-interaction of the C_{Te} and the adjacent N atoms.

2.2. Transition metal complexes

The availability of the free chelating bulky $\mathbf{L^{mes}}$ and $\mathbf{L^{DiPP}}$ ligands prompted us to carry out some preliminary explorations of their scope by means of the synthesis of representative examples of transition metal complexes. It is known that the coordination of the free chelating dicarbene ligands reported previously [6,7] with group 10 metal centres (Ni^{2+}, Pd^{2+}) leads to homoleptic complexes of ligand-to-metal stoichiometry 2:1 due to the kinetic control of the initial complexation reaction and the fact that strong metal-NHC bonds in combination with the chelate effect slow down ligand dissociation and redistribution. Therefore, the chemoselectivity of the $\mathbf{L^{DiPP}}$ and $\mathbf{L^{mes}}$ towards formation of complexes of 1:1 stoichiometry is a potentially attractive feature to consider.

Reactions of $\mathbf{L^{DiPP}}$ with one equiv. of [Pd(tmeda)Me_2] (tmeda is N, N, N′, *N*-tetramethylethylenediamine) or 0.5 equiv. of $[Pt(\mu\text{-}SMe_2)Me_2]_2$ resulted to the clean formation of the complexes $\mathbf{[Pd(L^{DiPP})Me_2]}$ and $\mathbf{[Pt(L^{DiPP})Me_2]}$, respectively. The complexes were characterised analytically, and by NMR spectroscopy. The ^{1}H-NMR spectrum indicates highly symmetric structures in solution as evidenced by the presence of two doublets and one septet for the *iso*propyl groups of the DiPP substituents. However, the solid-state structures determined crystallographically (see Figs. 4 and 5 for complexes **1** and **2**, respectively) indicate lower symmetry, originating from the puckered six membered chelating ring.

The bond lengths and angles are similar to those previously observed for analogous species [3a,11]. However, it is interesting to comment on a trend of M-CH_3 and M-C_{NHC} bond lengths in these very similar species: in the Pd complex **1**, the lengths of the two types of bonds are almost equal (within the measured e.s.d.s) but in the Pt complex **2** the C_{NHC} bonds are significantly shorter than the Pt-CH_3 bonds. This may imply a different balance of σ- and π-bond components for the two types of bonds but detailed understanding is not yet possible. The only other Pt dimethyl complex with a ligand of type **A** (R = Bu^t) (Scheme 1) was recently reported [3a] in conjunction with its reactivity toward CO_2; it was prepared by transmetallation from Ag to Pt. Bis-alkynyl complexes with a ligand of type **A** (R = C_6H_{11}) were studied in relation to their luminescence properties; they were prepared by direct metallation of the imidazolium salts with $PtCl_2$ in the presence of NaOAc, followed by reaction of the halides with alkynes [5b]. Pd dimethyl complexes with $\mathbf{L^{mes}}$ have been previously prepared by in situ deprotonation of the salt $\mathbf{(L^{mes}H_2)Br_2}$ [3c] but not structurally characterised.

Reactions of $\mathbf{L^{DiPP}}$ with 0.5 equiv. of $[Ir(1,5\text{-}COD)(\mu\text{-}Cl)]_2$ followed by anion exchange with KPF_6 gave complex **3**, which was characterised analytically, spectroscopically and crystallographically. In contrast to **1** and **2**, the ^{1}H NMR spectrum of **3** showed a non-symmetrical structure in solution as supported by the presence of four doublets and two septets for the *iso*propyl groups of the DiPP substituent. The non-symmetrical structure is also seen in the solid

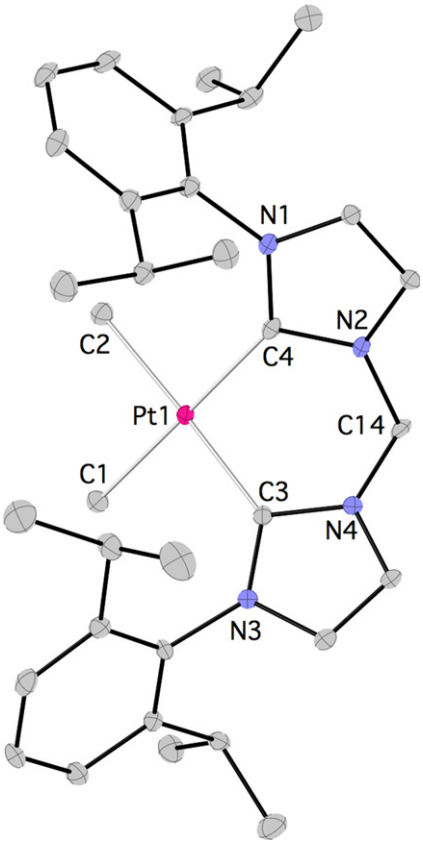

Fig. 5. Representation of the structure of **2**; ellipsoids are at 30% probability level. One THF molecule in the asymmetric unit is omitted for clarity. Selected bond lengths (Å) and angles (deg): C1–Pt1 2.088(5), C2–Pt1 2.088(5), C3–Pt1 2.037(5), C4–Pt1 2.020(5), C3–N3 1.367(6), N4–C3 1.372(6), C4–N1 1.390(6), N2–C4 1.380(5), N3–C3–N4 102.3(4), C2–Pt1–C1 85.35(19), N2–C4–N1 100.4(4), C3–Pt1–C1 93.43(18), C4–Pt1–C3 88.15(17), C4–Pt1–C2 93.14(18).

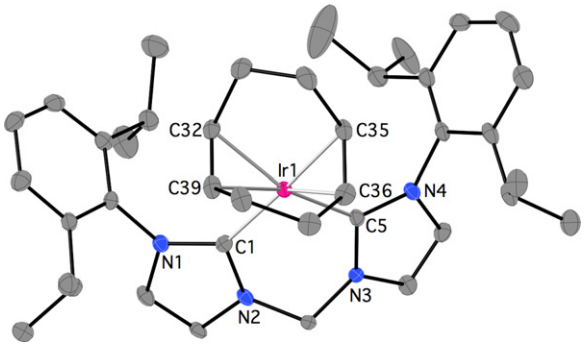

Fig. 6. Representation of the structure of the cation in **3**; ellipsoids are at 30% probability level. The anion $(PF_6)^-$ and one THF molecule in the asymmetric unit are omitted for clarity. Selected bond lengths (Å) and angles (deg): C1–N2 1.345(7), C1–N1 1.379(7), C1–Ir1 2.076(5), C5–N3 1.339(7), C5–Ir1 2.058(6), C32–Ir1 2.191(6), C35–Ir1 2.215(6), C5–N4 1.378(7), C39–Ir1 2.209(6), N2–C1–N1 103.1(5), N3–C5–N4 103.5(5), C5–Ir1–C1 87.4(2).

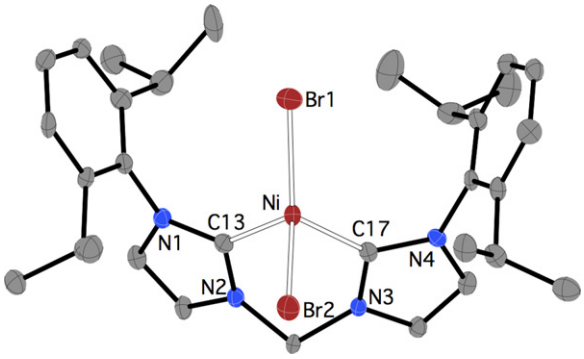

Fig. 7. Representation of the structure of **4**; ellipsoids are at 30% probability level. Selected bond lengths (Å) and angles (deg): Ni1–Br1 2.3501(10), Ni1–Br2 2.4009(10), C13–Ni1 1.976(7), C17–Ni1 = 1.975(6), N2–C13–N1 102.8(5), Br1–Ni1–Br2 123.00(4), C13–Ni1–Br2 102.75(17), C17–Ni1–Br2 96.92(16), C13–Ni1–Br1 115.20(18), C17–Ni1–C13 91.5(2).

state as depicted in the diagram of the cation (Fig. 6) obtained from a crystal structure determination of **3**.

The Ir centre adopts a distorted square planar geometry with virtually equal Ir–C_{NHC} bonds within the measured e.s.d.s. The Ir–C_{COD} bond lengths fall into the range 2.165–2.216 Å and there is elongation of the coordinated olefinic bonds due to increased back-bonding from the electron rich metal due to the strong σ-donor ability of the coordinated NHCs. Complex **3** is the first example of Ir^{I} centre with ligands of the type shown in Scheme 1. Two examples of Ir^{III} complexes with ligands of type **A** (R = Pr^{i}) have been obtained by the deprotonation of the corresponding bis-imidazolium salts with NaOAc or Et_3N in the presence of $[Ir(1,5\text{-COD})(\mu\text{-Cl})]_2$ and $[Cp^*IrCl(\mu\text{-Cl})]_2$, in processes that may also involve C–H activation of the C2-H by the Ir center [12]. The catalytic activity of **3** is currently under investigation.

Finally, $\mathbf{L^{DiPP}}$ was reacted with $[NiBr_2(dme)]$ in THF to afford the pink, paramagnetic tetrahedral complex **4**, which was characterised by analytical and X-ray diffraction methods. The analytical data support a ligand-to-metal stoichiometry of 1:1. Unfortunately, the crystals obtained were invariably of small size, which in combination with the low solubility of **4** in inert solvents (a fact that eliminates controlled recrystallisations, see Experimental Section) hampered an accurate crystal structure determination. Eventually a data set obtained at the synchrotron X-ray facility, Daresbury, UK, was adequate for solution and satisfactory refinement of the model, which established unequivocally the atom connectivity in the complex and its essential geometrical and metrical features (Fig. 7).

The Ni centre is in a distorted tetrahedral geometry with wide Br–Ni–Br (123.00(4)°) and relatively small C_{NHC}–Ni–C_{NHC} (91.5(2)°) angles. The Ni–C_{NHC} bonds fall in the long end of the observed range (average 1.90 Å, range 1.85–2.08 Å).

In view of the thermal and air sensitivity of $\mathbf{L^{DiPP}}$, which may limit its use for the synthesis of the interesting complex **4**, we developed a methodology based on the in situ deprotonation of the imidazolium salt $\mathbf{(L^{DiPP}H)_2Br_2}$ with $KN(SiMe_3)_2$. However, the low solubility of **4** in the reaction medium resulted in its contamination with KBr, the salt metathesis product from the deprotonation. Unexpectedly, purification of the mixture of **4** with KBr

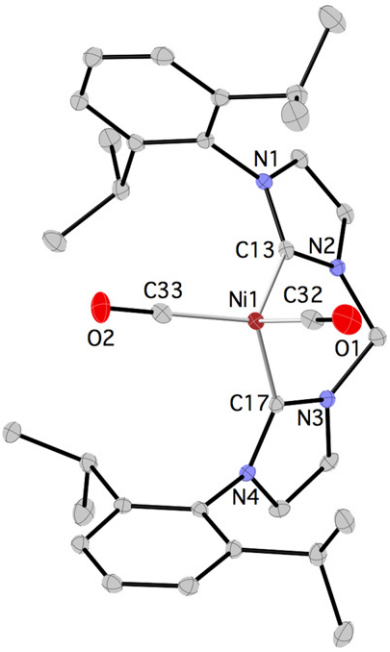

Fig. 8. Representation of the structure of **5**; ellipsoids are at 30% probability level. Selected bond lengths (Å) and angles (deg): C17–Ni1 1.955(2), C13–Ni1 1.957(2), C32–Ni1 1.759(3), C33–O2 1.158(3), C32–O1 1.159(3), C33–Ni1 1.764(2), C32–Ni1–C33 111.16(11), C32–Ni1–C17 112.93(10), C33–Ni1–C17 113.18(10), C32–Ni1–C13 113.68(10), C33–Ni1–C13 112.65(10), C17–Ni1–C13 92.06(9).

could be carried out by quick washing with degassed water on a glass sinter followed by quick drying giving analytically pure **4**. The observed selectivity for the formation of the complex of 1:1 metal-to-ligand stoichiometry as observed with **4** should be contrasted with the other Ni^{II} complexes with ligands of type A in Scheme 1, where the preferred products are square planar species of 1:2 metal-to-ligand stoichiometry and may be ascribed to the steric requirements of $\mathbf{L^{DiPP}}$.

Preliminary reactivity studies showed that **4** could be reduced in the presence of CO to the $[Ni(L^{DiPP})(CO)_2]$, a Ni^0 complex, which was structurally characterised (Fig. 8).

Here too, the metal is in a tetrahedral environment with C_{NHC}–Ni–C_{NHC} angle of 92.06(9)° very similar to the one observed in **4**. This value may relate to the $\mathbf{L^{DiPP}}$ ligand natural bite angle [13]. The Ni–C_{NHC} bond lengths are marginally shorter than in **4** while the Ni–C_{CO} are shorter than the Ni–C_{NHC} bonds indicating a good degree of π-back-bonding.

3. Conclusions

A method for the synthesis of free 1,1′-methylene-bis-(3-aryl-imidazol-2-ylidene) ligands of high purity and in synthetically useful quantities will provide alternative or complementary routes for the synthesis of organometallic complexes that are sensitive to strong bases or the oxidising conditions of transmetallation from silver. This idea has been exemplified in this work by the synthesis of some novel organometallics of group 10 and Ir metals that were either not previously accessible or via multistep synthetic schemes. We expect that this development will open the way for the more widespread use of 1,1′-methylene-bis-(3-aryl-imidazol-2-ylidene) ligands across the Periodic Table.

4. Experimental

4.1. General

All manipulations were performed under nitrogen in a MBraun glovebox or using standard Schlenk techniques, unless stated otherwise. Solvents were dried using standard methods and distilled under nitrogen prior use. The light petrol used throughout had a b.p. of 40 to 60 °C. The starting materials were obtained from commercial sources or prepared by modification of the literature procedures as follows: crude, usually colored bis-imidazolium $\mathbf{(L^{mes}H_2)Br_2}$ [8] and $\mathbf{(L^{DiPP}H_2)Br_2}$ [7], were washed with minimum amount of acetone to afford colorless powders that were dried under vacuum and finally azeotropically with toluene. The salt $\mathbf{(L^{DiPP}H_2)(OTf)_2}$ that was prepared to facilitate crystallographic characterisation of the bis-imidazolium cation, was obtained by anion exchange from $\mathbf{(L^{DiPP}H_2)Br_2}$, with NaO_3SCF_3 in CH_2Cl_2 and crystallised from CH_2Cl_2/petrol; $[Pd(tmeda)Me_2]$ [14] and $[PtMe_2(\mu\text{-}SMe_2)]_2$[15] were prepared according to literature methods.

Elemental analyses were carried out by the London Metropolitan University microanalytical laboratory. NMR data were recorded on Bruker AV-300 and DPX-400 spectrometers, operating at 300 and 400 MHz (^{1}H), respectively. The spectra were referenced internally using the signal from the residual protio-solvent (^{1}H) or the signals of the solvent (^{13}C).

4.1.1. 1,1′-methylene-bis-(3-diisopropylphenyl-imidazol-2-ylidene) L^{DiPP}

$\mathbf{(L^{DiPP}H_2)Br_2}$ (2.50 g, 4.00 mmol) was weighed out into a Schlenk and suspended in diethyl ether (30 ml). In a separate Schlenk, $KN(SiMe_3)_2$ (1.74 g, 8.70 mmol) was dissolved in diethyl ether (20 ml). The solution of $KN(SiMe_3)_2$ was cooled to -78 °C and added portionwise with efficient stirring to the suspension of the salt at the same temperature, the suspension turning cream upon full addition. The mixture was stirred at -78 °C for 1 h and allowed to warm to –30 °C slowly over 2 h and stirred at this temperature for 30 min. At this point a light yellow suspension is formed. The reaction mixture was filtered through Celite into a cold (–30 °C) receiver flask. The precipitate was washed with cooled (–20 °C) diethyl ether (4 × 50 ml). The solvent was removed under reduced pressure to give a lemon yellow solid, which was spectroscopically pure. Yield: 1.46 g, 78%. NMR (C_6D_6): ^{1}H, δ_H 1.10, 1.30 (2 × 6H, d, $CH(CH_3)_2$, J = 7.32 Hz), 2.80 (2H, septet, $CH(CH_3)_2$, J = 7.32 Hz), 6.30 (2H, s, CH_2 bridge), 6.50 (2H, s, 5-imidazol-2-ylidene), 7.20 (2H, s, backbone imidazol-2-ylidene), 7.20 (4H, d, aromatic DiPP, J = 7.32), 7.30 (2H, t, aromatic DiPP, J = 7.32). $^{13}C\{^1H\}$: δ_C, 23.7, 24.5 (^{i}Pr CH_3), 28.5 (^{i}Pr $C(CH_3)_2$), 65.6 (-CH_2-), 118.1, 122.8 (4,5-imidazol-2-ylidene), 128.3, 128.9, 132.0, 146.2 (aromatic),

218.9 (imidazol-2-ylidene). The solid can be stored at −35 °C under nitrogen without decomposition.

4.1.2. 1,1′-methylene-bis-(3-mesityl-imidazol-2-ylidene) L^{mes}

($L^{mes}H_2$)Br_2 (1.50 g, 2.75 mmol) was weighed out into a Schlenk and suspended in ether (30 ml). In a separate Schlenk, $KN(SiMe_3)_2$ (1.20 g, 6.05 mmol) was dissolved in diethyl ether (20 ml). The solution of $KN(SiMe_3)_2$ was cooled to −78 °C and added portionwise with efficient stirring to the suspension of the salt at the same temperature. After completion of the addition, the mixture was stirred at −78 °C for 1 h and allowed to warm to −20 °C slowly over 2 h and stirred at this temperature for 30 min. The solution was filtered through a pad of Celite (2 cm) into a Schlenk that was kept at −78 °C. The pad was washed with pre-cooled diethyl ether until the washings were not colored (2 × 30 ml). The combined washings were concentrated under reduced pressure to *ca.* 1/3 of the original volume and the solution was cooled at −35 °C affording a yellow solid that was isolated by decanting the mother liquor with a cannula and washed with petrol (30 ml) and dried under vacuum. Yield: 0.62 g, 60.5%. NMR (C_6D_6): ^1H, δ_H 2.10 (12H, s, *o*-C*H*$_3$), 2.20 (6H, s, *p*-C*H*$_3$), 6.30 (2H, s, C*H*$_2$), 6.40 (2H, s, backbone imidazol-2-ylidene), 6.80 (4H, s, mesityl aromatic-H), 7.20 (2H, s, backbone imidazol-2-ylidene). $^{13}C\{^1H\}$: δ_C, 17.9, 20.9 (mesityl-CH_3), 65.7 (-CH_2-), 118.1, 121.7 (4,5-imidazol-2-ylidene), 129.0, 135.3, 137.3, 138.9 (aromatic), 218.0 (imidazol-2-ylidene). The solid can be stored at −35 °C under nitrogen without decomposition. X-ray quality crystals were obtained by prolonged cooling of ether solutions at −35 °C.

4.1.3. Preparation of $L^{DiPP}S_2$

Oven dried sulphur (0.02 g, 0.64 mmol) in THF (20 ml) was added to **L^{DiPP}** (0.15 g, 0.32 mmol) in THF (30 ml) at RT. The mixture was stirred for 72 h to give a pale orange solution. The THF was evaporated under reduced pressure, the solid residue was dissolved in ether (30 ml) and layered with petrol (30 ml). The pale orange solid precipitate was collected and dried under vacuum. NMR (C_6D_6): ^1H, δ_H 0.90 and 1.20 (d, 2 × 12H, (C*H*$_3$)$_2$CH), 2.50 (sept, 4H, (CH_3)$_2$C*H*), 5.80 (s, 2H, backbone imidazol-2-ylidene), 6.00 (s, 2H, methylene bridge), 7.00 (doublet, 4H, aromatic DiPP), 7.10 (triplet, 2H, arom. DiPP), 7.50 (s, 2H, backbone imidazol-2-ylidene). $^{13}C\{^1H\}$: δ_C 22.3 and 22.9 ((*C*H$_3$)$_2$CH), 27.5 ((*C*H$_3$)$_2$CH), 54.6 (*C*H$_2$ bridge), 116.6 and 117.4 (imidazol-2-ylidene backbone), 123.0, 128.9, 132.9 and 145.4 (aromatic), 180.3 (*C* = S). Anal. Calcd for $C_{31}H_{40}N_4S_2$ (%): C, 69.88; H 7.57; N 10.52; found (%): C, 69.78; H, 7.64; N, 10.43.

4.1.4. Preparation of $L^{DiPP}Se_2$

Dried selenium (0.05 g, 0.64 mmol) in THF (20 ml) was added to a stirred solution of **L^{DiPP}** (0.15 g, 0.32 mmol) in THF (30 ml) at RT. The mixture was stirred at RT for 72 h to giving a pale green/brown solution. The volatiles were removed under reduced pressure and the solid residue dissolved in ether (30 ml). Small amounts of black precipitate were removed by filtration and the filtrate evaporated to dryness giving a dark orange solid. NMR (C_6D_6): ^1H, δ_H 0.90 and 1.20 (2 d, 24H, (C*H*$_3$)$_2$CH), 2.40 (sept, 4H, (CH_3)$_2$C*H*), 5.90 [(s, 2H, imidazol-2-ylidene), 6.30 (s, 2H, C*H*$_2$ bridge), 7.00 (d, 4H, aromatic), 7.10 (t, 2H, aromatic)], 8.00 (s, 2H, imidazol-2-ylidene). $^{13}C\{^1H\}$: δ_C, 22.3 and 23.0 ((*C*H$_3$)$_2$CH), 27.7 ((*C*H$_3$)$_2$CH), 57.9 (*C*H$_2$ bridge), 118.8 and 119.4 (backbone imidazol-2-ylidene), 123.0, 129.0, 133.5 and 145.0 (aromatic), 161.3 (*C* = Se). Anal. Calcd for $C_{31}H_{40}N_4Se_2$ (%): C, 59.42; H 6.43; N 8.94; found (%): C, 58.22; H, 7.13; N, 8.72.

4.1.5. Preparation of $L^{DiPP}Te_2$

Tellurium (0.08 g, 0.64 mmol) in THF (20 ml) was added to a stirred solution of **L^{DiPP}** (0.15 g, 0.32 mmol) in THF (30 ml) at RT. After 72 h, a brown solution was obtained. The THF was removed under vacuum and the solid residue was dissolved in diethyl ether (30 ml). Some black precipitate formed on addition of ether was removed by filtration. The filtrate was layered with petrol to give yellow brown crystals. NMR (C_6D_6): ^1H, δ_H, 0.80 and 1.30 (two d, 24H, (C*H*$_3$)$_2$CH), 2.30 (sept, 4H, (CH_3)$_2$C*H*), 6.10 (s, 2H, imidazol-2-ylidene), 6.40 (s, 2H, methylene bridge protons), 7.00 (d, 4H, aromatic), 7.10 (t, 2H, aromatic), 8.6 (s, 2H, imidazol-2-ylidene). $^{13}C\{^1H\}$: δ_C, 22.1 and 23.3 ((*C*H$_3$)$_2$CH), 27.9 ((*C*H$_3$)$_2$CH), 64.0 (*C*H$_2$ bridge), 121.3 and 121.4 (imidazol-2-ylidene), 123.2, 129.3, 133.5 and 144.7 (aromatic). *C* = Te was not observed. Anal. Calcd for $C_{31}H_{40}N_4Te_2$ (%): C, 55.43; H 5.57; N 7.74; found (%): C, 55.39; H, 5.66; N, 7.85. X-ray quality crystals were obtained by layering a C_6D_6 solution with petrol in an NMR tube.

4.1.6. Synthesis of [Pd$L^{DiPP}Me_2$] (1)

To a solution of [Pd(tmeda)Me_2] (0.10 g, 0.39 mmol) in diethyl ether at −78 °C, was added by cannula a solution of **L^{DiPP}** (0.18 g, 0.39 mmol) in the same solvent. Upon completion of the addition, the colour had changed from light to intense yellow. The solution was allowed to warm to room temperature overnight becoming brown-red. Evaporation of the solvent under reduced pressure left a dark green-purple solid, which was dissolved in THF and layered with petrol to give colorless crystals. NMR (acetone-d^6): ^1H, δ_H −1.00 (s, 6H, Pd-(C*H*$_3$)$_2$), 0.90 (d, 12H, (C*H*$_3$)$_2$CH), 1.10 (d, 12H, (C*H*$_3$)$_2$CH), 1.60 (m, 4H, THF), 2.60 (sept, 4H, (CH_3)$_2$C*H*), 6.15 (s, 2H, C*H*$_2$ bridge), 6.85 (s, 2H, NHC backbone), 7.10 (d, 4H, DiPP), 7.20 (d, 2H, DiPP), 7.40 (s, 2H, NHC backbone). $^{13}C\{^1H\}$: δ_C −3.8 [Pd-(CH_3)$_2$], 23.8 ((*C*H$_3$)$_2$CH on Dipp), 25.6 ((*C*H$_3$)$_2$CH), 55.0 ((*C*H$_3$)$_2$CH), 70.0 (*C*H$_2$ bridge), 120.0 (imidazol-2-ylidene), 123.8 (imidazol-2-ylidene backbone), 125.0 (C = C backbone), 126.3 (aromatic of DiPP), 130.0 (aromatic of DiPP), 146.3 (aromatic of DiPP), 212.0 (C_{NHC}). Anal. Calcd. for $C_{33}H_{48}N_4Pd$.THF (%): C, 65.60; H 8.30; found (%): C, 65.62; H, 8.35.

4.1.7. Synthesis of [Pt$L^{DiPP}Me_2$] (2)

To a solution of [(Pt(μ-SMe_2)$_2$$Me_2$]$_2$ (0.04 g, 0.07 mmol) in diethyl ether at −78 °C, was added by cannula a solution of **L^{DiPP}** (0.07 g, 0.14 mmol) in the same solvent. After stirring for 72 h the volatiles were removed under reduced pressure to give a black solid residue which was washed with pentane and ether and dissolved in THF giving a

purple solution which on concentration and standing at room temperature overnight gave colorless crystals. More crystals could be obtained from the supernatant by layering it with petrol. NMR (acetone-d^6): ^{1}H, δ_H -0.10 (t, 6H, (C*H*$_3$)$_2$-Pt satellites), 1.25 (d, 12H, (C*H*$_3$)$_2$CH), 1.50 (doublet, 12H, (C*H*$_3$)$_2$CH), 2.00 (m, 4H, THF), 3.05 (sept, 4H, (CH$_3$)$_2$C*H*), 3.85 (4H, m, THF), 6.30 (s, 2H, C*H*$_2$ bridge), 7.20 (s, 2H, NHC backbone), 7.40 (d, 4H, aromatic DiPP), 7.55 (d, 2H, aromatic DiPP), 7.70 (s, 2H, NHC backbone). Anal. Calcd. for $C_{33}H_{48}N_4Pt{\cdot}THF$ (%): C, 57.90; H 7.30; N, 7.29; found (%): C, 57.93; H, 7.00; 7.19.

4.1.8. Synthesis of [IrL^{DiPP}(1,5-COD)]PF$_6$ (3)

A solution of **L^{DiPP}** (0.11 g, 0.24 mmol) in THF (20 ml) was added at −78 °C to a solution of [Ir(1,5-COD)(μ-Cl)]$_2$ (0.08 g, 0.12 mmol) in the same solvent (10 ml). After the addition the cooling bath was removed and the orange reaction mixture was allowed to reach room temperature, when it became brown. A suspension of KPF$_6$ (0.02 g, 0.12 mmol) in THF (20 ml) was then added to the reaction mixture and the whole was stirred at room temperature overnight. After evaporation of the volatiles under reduced pressure, the solid residue was washed with petrol (2 × 15 ml) and toluene (15 ml) and crystallised from THF/petrol affording dark red crystals. NMR (acetone-d^6): ^{1}H, δ_H 7.95 (d, 2H, NC*H*CHN), 7.66 (d, 2H, NCHC*H*N), 7.50–7.60 (m, 2H, DiPP aromatic), 7.35–7.50 (m, 4H aromatic DiPP), 6.68 (d, 1H, CH$_2$ bridge), 6.52 (d, 1H, CH$_2$ bridge), 4.29 (br s, 4H, COD vinyl), 3.58 (m, THF), 3.20 (br s, 8H, COD allyl), 2.84 (sept, C*H*(CH3)2), 2.24 (sept, C*H*(CH$_3$)$_2$), 1.48 (d, 3H, CH(C*H*$_3$)$_2$), 1.39 (d, 3H, CH(C*H*$_3$)$_2$), 1.11 (d, 3H, CH(C*H*3)2), 0.98 ppm (d, 3H, CH(C*H*$_3$)$_2$); ^{13}C{^{1}H}: δ_C 172.7 (NCN), 136.4, 131.5, 127.3, 125.2, 121.5 (aromatic DiPP), 73.2 (COD vinyl), 68.1 (CH$_2$ bridge), 63.9 (iPr CH), 31.8, 26.2 (iPr CH3) ppm; ^{19}F NMR: −72.4 (d). Anal. Calcd. for $C_{39}H_{43}F_6IrN_4P$ (%): C, 51.76; H, 4.79; N, 6.19; found: C, 51.66; H, 4.77; N, 6.16.

4.1.9. Preparation of [NiL^{DiPP}Br$_2$] (4)

L^{DiPP} (0.15 g, 0.32 mmol) in THF (30 ml) was added at −78 °C with stirring to [NiBr$_2$(dme)] (0.10 g, 0.32 mmol) in THF (30 ml). Stirring at −78 °C was continued for 10 min and then the mixture was allowed to warm to room temperature when it became dark orange. The volatiles were removed under reduced pressure to give a pink solid, which was insoluble in inert solvents but sparingly soluble in THF. X-ray quality crystals were obtained by dissolving a small amount in THF (30 ml) and layering with diethyl ether.

4.1.10. Preparation of [NiL^{DiPP}Br$_2$] (4) by generating the L^{DiPP} in situ

KN(SiMe$_3$)$_2$ (2.40 g, 12.00 mmol) in diethyl ether (100 ml) was added at −78 °C portionwise with rapid stirring to (**L^{DiPP}H$_2$)Br$_2$** (3.00 g, 4.80 mmol) in diethyl ether (100 ml). This was followed by addition at the same temperature of [NiBr$_2$(dme)] (0.11 g, 3.70 mmol, equimolar amount based on 75% carbene yield) in THF (100 ml). Cold THF (200 ml at −78 °C) was used to dilute the reaction mixture. The mixture was allowed to warm to room temperature and then stirred overnight. A brown

Table 1
X-ray data collection and refinement parameters for compounds (**L^{DiPP}H$_2$)(OTf)$_2$**, **L^{mes}**, **L^{DiPP}Te^2** and complexes **1–5**.

	(L^{DiPP}H$_2$)(OTf)$_2$	L^{mes}	L^{DiPP}Te$_2$	1	2	3	4	5
Chemical formula	$C_{33}H_{42}F_6N_4O_6S_2$	$C_{25}H_{28}N_4$	$C_{37}H_{40}D_6N_4Te_2$	$C_{37}H_{54}N_4OPd$	$C_{37}H_{54}N_4OPt$	$C_{39}H_{52}IrN_4P$ $F_6C_4H_8O$	$C_{31}H_{40}Br_2N_4Ni$	$C_{37}H_{48}N_4Ni$ O_3
CCDC number	906016	906017	906018	906019	906020	906021	906022	906023
Formula mass	768.83	384.5	808.01	2708.97	765.93	986.12	687.20	655.50
Crystal system	Monoclinic	Monoclinic	Monoclinic	Orthorhombic	Orthorhombic	Orthorhombic	Orthorhombic	Monoclinic
a/Å	15.6001(11)	8.030(3)	12.1082(10)	9.2015(18)	9.16850(10)	13.6258(4)	12.6116(13)	10.4866(3)
b/Å	24.6198(11)	9.795(3)	16.4200(13)	18.932(4)	18.9619(2)	24.9908(7)	14.5499(15)	17.4528(4)
c/Å	9.9798(4)	28.373(10)	18.3694(15)	19.892(4)	19.9278(2)	25.1385(4)	16.8485(17)	19.3943(6)
α/°	90.00	90.00	90.00	90.00	90.00	90.00	90.00	90.00
β/°	103.562(4)	97.544(3)	99.721(2)	90.00	90.00	90.00	90.00	104.482(1)
γ/°	90.00	90.00	90.00	90.00	90.00	90.00	90.00	90.00
Volume/Å^3	3726.1(4)	2212.3(13)	3599.7(5)	3465.2(12)	3464.49(6)	8560.2(4)	3091.7(5)	3436.77(16)
Temp/K	120(2)	120(2)	120(2)	120(2)	120(2)	153(2)	120(2)	120(2)
Space group	$C2/c$	$P\,2_1/c$	$P2_1/c$	$P2_12_12_1$	$P2_12_12_1$	$Pbca$	$P2_12_12_1$	$P2_1/n$
Z	4	4	4	4	4	8	4	4
μ/mm^{-1}	0.220	0.069	1.650	–	0.9228	0.597	3.238	0.605
Reflections measured	26333	21165	57802	36753	30465	67631	18813	44020
Independent reflections	3291	6380	8380	10304	7809	8381	4280	7853
R_{int}	0.1010	0.0524	0.0671	0.0449	0.0450	0.0459	0.0477	0.0836
Final R_1 values ($I > 2\sigma(I)$)	0.2005	0.0539	0.0508	0.0309	0.0306	0.0734	0.0401	0.0482
Final $wR(F^2)$ values ($I > 2\sigma(I)$)	0.1217	0.1502	0.1038	0.0695	0.0609	0.1155	0.0974	0.0946
Final R_1 values (all data)	0.2101	0.0625	0.0684	0.0331	0.0348	0.0459	0.0401	0.0823
Final $wR(F^2)$ values (all data)	0.2101	0.1601	0.1143	0.0711	0.0628	0.0734	0.1016	0.1070
Goodness of fit on F^2	1.216	1.035	1.104	1.019	1.130	1.046	1.070	1.037

suspension with some pink precipitate was observed. The mixture was filtered on a glass sinter and washed with degassed H_2O (30 ml) followed by EtOH (30 ml) and then Et_2O (50 ml). The dark pink solid was dried under vacuum. Anal. Calcd. for $C_{31}H_{40}N_4Br_2Ni$ (%): C, 54.18; H, 5.87; N, 8.15; found: C, 54.01, H, 5.74; N, 8.03. The product is paramagnetic giving featureless NMR spectra in THF-d^8.

4.1.11. Formation of [NiL^{DiPP}(CO)$_2$] **(5)**

In a Fisher-Porter bottle, to a solution of [NiL^{DiPP}Br$_2$] (0.04 g, 0.06 mmol) in THF (10 ml) was added Na/Hg (1.00 g of 0.4% w/w, excess), the mixture was pressurised with CO (100 psi), and stirred at room temperature for 12 h. After releasing of the pressure the solution was decanted from the Hg pool and the THF removed under reduced pressure. The residue was dissolved in ether, filtered, the filtrate concentrated and cooled (4 °C) to give small quantity of yellow crystals that were characterised crystallographically.

4.1.12. X-ray crystallography

The data sets for **(L^{DiPP}H$_2$)(OTf)$_2$** and complexes **2**, **3** and **5** were collected on a Enraf-Nonius Kappa CCD area detector diffractometer with an FR591 rotating anode (Mo Kα radiation) and an Oxford Cryosystems low-temperature device, operating in ω scanning mode with ψ and ω scans to fill the Ewald sphere. The crystals were mounted on a glass fiber with silicon or fluorocarbon grease, from Fomblin vacuum oil. The programs used for control and integration were Collect, Scalepack, and Denzo [16]. All solutions and refinements were performed using the WinGX [17] package and all software packages within. All non-hydrogen atoms were refined using anisotropic thermal parameters, and hydrogens were added using a riding model. Complexes **1**, **2**, **3** and **5** contain one THF solvent molecule of crystallization in the asymmetric unit. In the structures of **(LDiPPH$_2$)(OTf)$_2$** and **3** one of the isopropylphenyl groups was disordered over two positions that were refined anisotropically without any restraints. The structure of **1** contains one THF solvent molecule of crystallization which was disordered over two positions and refined anisotropically. The crystals of **L^{mes}**, **L^{DiPP}Te$_2$** and of the complexes **1** and **4** were very small, and the data sets were collected at the synchrotron facility at Darebury, UK [18]. Crystal data for all structurally characterised compounds are given in Table 1.

Acknowledgements

We thank CNRS for a fellowship (to AAD). AAD is also grateful to the Région Alsace, the Département du Bas-Rhin and the Communauté urbaine de Strasbourg for the award of a Gutenberg Excellence Chair (2010–2011). We also thank Dr Pierre Braunstein for support and fruitful discussions and Dr Mark E. Light, Dr Simon J. Coles (University of Southampton) and Dr Pierre de Fremont (Laboratoire de chimie de coordination, UMR 7177) for the data collection of **L^{mes}** and **4** and assistance in structure solution and refinement, respectively.

Appendix. Supplementary material

Supplementary material associated with this article can be found at http://www.sciencedirect.com, at http://dx.doi.org/10.1016/j.crci.2013.01.016.

References

[1] A.J. Arduengo, R.L. Harlow, M. Kline, J. Am. Chem. Soc. 113 (1991) 361.
[2] W.A. Herrmann, M. Elison, J. Fischer, C. Köcher, G.R.J. Artus, Angew. Chem. Int. Ed. Engl. 34 (1995) 2371.
[3] (a) S. Jamali, D. Milic, R. Kia, Z. Mazloomi, H. Abdolahi, Dalton Trans. 40 (2011) 9362 ;
(b) A.D. Yeung, P.S. Ng, H.V. Huynh, J. Organomet. Chem. 696 (2011) 112 ;
(c) S.S. Subramanium, L.M. Slaughter, Dalton Trans. (2009) 6930 ;
(d) T. Scherg, S.K. Schneider, G.D.J. Frey, R. Schwarz, E. Herdtweck, W.A. Herrmann, Synlett (2006) 2894 ;
(e) S. Budagumpi, R.A. Haque, A.W. Salman, Coord. Chem. Rev. 256 (2012) 1787 ;
(f) R. Corberán, E. Mas-Marzá, E. Peris, Eur. J. Inorg. Chem. (2009) 1700 ;
(g) M. Muehlhofer, T. Strassner, W.A. Herrmann, Angew. Chem. Int. Ed. 41 (2002) 1745.
[4] (a) A.S. McCall, H. Wang, J.M. Desper, S. Kraft, J. Am. Chem. Soc. 133 (2011) 1832 ;
(b) D. Meyer, S. Ahrens, T. Strassner, Organometallics 29 (2010) 3392.
[5] (a) Y. Unger, A. Zeller, M.A. Taige, T. Strassner, Dalton Trans. 38 (2009) 4786 ;
(b) Y. Zhang, J.A. Garg, C. Michelin, T. Fox, O. Blacque, K. Venkatesan, Inorg. Chem. 50 (2011) 1220 ;
(c) K. Li, X. Guan, C.W. Ma, W. Lu, Y.C.M. Chen Che, Chem. Commun. 47 (2011) 9075.
[6] (a) R.E. Douthwaite, D. Häussinger, M.L.H. Green, P.J. Silcock, P.T. Gomes, A.M. Martins, A.A. Danopoulos, Organometallics 18 (1999) 4584 ;
(b) T.A.P. Paulose, S.C. Wu, J.A. Olson, T. Chau, N. Theaker, M. Hassler, J.W. Quail, S.R. Foley, Dalton Trans. 41 (2012) 251.
[7] K.A. Kreisel, G.P.A. Yap, K.H. Theopold, Organometallics 25 (2006) 4670.
[8] M.G. Gardiner, W.A. Herrmann, C.P. Reisinger, J.R. Schwarz, M. Spiegler, J. Organomet. Chem. 572 (1999) 239.
[9] S. Ahrens, T. Strassner, Inorg. Chim. Acta. 359 (2006) 4789.
[10] A.J. Arduengo, F. Davidson, H.V.R. Dias, J.R. Goerlich, D. Khasnis, W.J. Marshall, T.K. Prakasha, J. Am. Chem. Soc. 119 (1997) 12742.
[11] A.A.D. Tulloch, S. Winston, A.A. Danopoulos, G. Eastham, M.B. Hursthouse, Dalton Trans. (2003) 699.
[12] (a) M. Albrecht, J.R. Miecznikowski, A. Samuel, J.W. Faller, R.H. Crabtree, Organometallics 21 (2002) 3596 ;
(b) M. Vogt, V. Pons, D.M. Heinekey, Organometallics 24 (2005) 1832.
[13] P. Dierkes, P.W.N.M. van Leeuwen, J. Chem. Soc. Dalton Trans. 28 (1999) 1513.
[14] W. De Graaf, J. Boersma, W.J.J. Smeets, A.L. Spek, G. Van Koten, Organometallics 8 (1989) 2907.
[15] G.S. Hill, M.J. Irwin, C.J. Levy, L.M. Rendina, R.J. Puddephatt, R.A. Andersen, L. McLean, Inorganic Syntheses, John Wiley & Sons Inc., 1998 , pp. 149.
[16] Z. Otwinoski, W. Minor, Methods Enzymol 276 (1997) 307.
[17] L.J. Farrugia, J. Appl. Crystallogr. 32 (1999) 83.
[18] R.J. Cernik, W. Clegg, C.R.A. Catlow, G. Bushnell-Wye, J.V. Flaherty, G.N. Greaves, M. Hamichi, I. Burrows, D.J. Taylor, S.J. Teat, J. Synchrotron Radiat. 4 (1997) 279.